

# Analytical Methods

Accepted Manuscript



This is an *Accepted Manuscript*, which has been through the Royal Society of Chemistry peer review process and has been accepted for publication.

*Accepted Manuscripts* are published online shortly after acceptance, before technical editing, formatting and proof reading. Using this free service, authors can make their results available to the community, in citable form, before we publish the edited article. We will replace this *Accepted Manuscript* with the edited and formatted *Advance Article* as soon as it is available.

You can find more information about *Accepted Manuscripts* in the [Information for Authors](#).

Please note that technical editing may introduce minor changes to the text and/or graphics, which may alter content. The journal's standard [Terms & Conditions](#) and the [Ethical guidelines](#) still apply. In no event shall the Royal Society of Chemistry be held responsible for any errors or omissions in this *Accepted Manuscript* or any consequences arising from the use of any information it contains.

1  
2  
3  
4  
5  
6  
7  
8  
9  
10  
11  
12  
13  
14  
15  
16  
17  
18  
19  
20  
21  
22  
23  
24  
25  
26  
27  
28  
29  
30  
31  
32  
33  
34  
35  
36  
37  
38  
39  
40  
41  
42  
43  
44  
45  
46  
47  
48  
49  
50  
51  
52  
53  
54  
55  
56  
57  
58  
59  
60

## Development of a Multicommuted Flow Analysis Procedures for Simultaneous Determination of Sulfate and Chloride in Petroleum Coke Employing a Homemade Syringe Pump and a LED-Based Photometer

Felisberto G. Santos<sup>1</sup>, Andréia C. Pereira<sup>1</sup>, Sandra M. Cruz<sup>2</sup>, Cezar A. Bizzi<sup>2</sup>,  
Érico M. M. Flores<sup>2</sup>, Boaventura F. Reis<sup>1\*</sup>

<sup>1</sup>Centro de Energia Nuclear na Agricultura, Universidade de São Paulo  
Av. Centenário, 303, São Dimas, CEP 13400 970 Piracicaba-SP, Brazil

<sup>2</sup>Departamento de Química, Universidade Federal de Santa Maria, Santa  
Maria, RS

### *Abstract*

The current paper deals with procedures for simultaneous determination of sulfate and chloride in petroleum coke samples after microwave-induced combustion (MIC), which were implemented employing a multicommuted flow analysis process. The setup comprised a homemade syringe pump and two individual flow system manifolds, each coupled to a homemade LED-based photometer. Dedicated software enabled sampling and reading steps to be performed while displacing the syringe pistons forward and backward, allowing a sampling rate of 150 determinations per hour. The procedure for sulfate determination was based on the reaction formation of barium with sulfate and turbidimetric detection, while the procedure for chloride determination was based on the photometric mercury/thiocyanate method. In order to investigate the feasibility of both the equipment setup and the proposed procedures, samples of petroleum coke previously digested by microwave induced combustion (MIC) were analyzed. For accuracy assessment, samples were also analyzed employing ion chromatography and inductively coupled plasma optical emission spectrometry to determine chloride and sulfate, respectively. The paired *t*-test indicated no significant difference between the results for our method and the established methods, at a 95% confidence level. Linear responses ( $r = 0.999$ ) were obtained with concentrations ranging from 10 to 700 mg L<sup>-1</sup> for sulfate, and from 0.25 to 10 mg L<sup>-1</sup> chloride.

### *Keywords*

Syringe pump, Multicommutated flow analysis, Petroleum coke, Chloride and sulfate, Light emitting diode photometer, Green chemistry, Microwave induced combustion.

## 1. Introduction

Petroleum coke, a byproduct of the thermal processing of crude oil, has a high carbon content, including condensed aromatic rings, making it a useful feedstock for the gasification process.<sup>1-5</sup> Petroleum coke has also been used as a carbon source for the aluminum, refractory, and metallurgical industries.<sup>6-8</sup> Sulfate and chloride are among the main inorganic contaminants present in crude oils<sup>9-11</sup> and consequently in heavy products such as petroleum coke.

During the industrial processing of petroleum coke, sulfur compounds are released into the atmosphere, resulting in environmental damage, including the corrosion of metallic surfaces.<sup>12,13</sup> This element, when released into the atmosphere, can cause an increase in the occurrence of acid rain.<sup>14,15</sup> Although chloride itself does not have negative effects on the environment, its presence in petroleum coke can impair coke quality for industrial use.<sup>9,11,16</sup> Thus, the determination of sulfate and chloride content in petroleum coke is essential to evaluate its appropriate use and its effect on the environment.

In samples of petroleum coke, chloride has been determined using inductively coupled plasma-optical emission spectrometry (ICP OES),<sup>6,9</sup> ion chromatography (IC)<sup>11</sup> and inductively coupled plasma mass spectrometry (ICP MS).<sup>9</sup> Sulfur has been also determined by ICP OES,<sup>6</sup> and using the method dictated in ASTM 5016.<sup>17</sup>

Techniques such as IC, ICP OES, and ICP MS, normally require the introduction of a dissolved sample. The fact that petroleum coke samples have a chemical resistance to acid oxidation, even when high temperatures and pressure are employed, complicates the sample preparation step.<sup>6,10,11</sup> Because the organic constituents of petroleum coke behave like fuel under a rich oxygen atmosphere, combustion techniques have been successfully used for petroleum coke digestion. When combustion is performed in closed vessels, as it is in microwave induced combustion (MIC), high sample masses can be digested, affording final digests with a low residual carbon content (RCC).<sup>6,11</sup> There is no

1  
2  
3 loss of volatile analytes, allowing the use of more dilute absorbing solutions,  
4 thus favoring the achievement of low limits of detection.

5  
6 The detection techniques discussed above are relatively expensive,  
7 making the development of analytical procedures based on less costly  
8 methodologies important. Flow injection analysis (FIA) is considered a suitable  
9 method for handling sample and reagent solutions for analytical purposes, and  
10 provides the relatively high throughput necessary for routine analysis.<sup>18-21</sup> The  
11 FIA approach has already been employed to determine sulfate in plant digests  
12 by turbidimetry<sup>22,23</sup> and chloride in cement and water by spectrophotometry.<sup>24,25</sup>

13  
14 In these cases, mercury thiocyanate and barium chloride are the  
15 reagents most commonly used. However, there are environmental restrictions  
16 to their use due to the environmental risks associated with the release of  
17 mercury and barium into the environment. According to green analytical  
18 chemistry guidelines (GAC),<sup>26,27</sup> if the use of an environmentally restricted  
19 reagent is inevitable, as little as possible should be used. This guideline is  
20 difficult to adhere, when the continuous pumping of reagent solutions, as is  
21 required for typical FIA systems, is employed.<sup>22-24</sup> However, the multicommuted  
22 flow analysis (MCFA) process may be a viable alternative. MCFA is a flow  
23 analysis approach in which sample and reagent solutions are inserted into the  
24 analytical path intermittently, allowing a significant reduction in reagent  
25 consumption and waste generation.<sup>28-31</sup>

26  
27 The most important aspect of a flow analysis system is the fluid  
28 propulsion process, which is usually performed using a peristaltic pump.<sup>32</sup> Other  
29 fluid propelling devices, such as solenoid mini-pumps<sup>33,34</sup> and multisyringes,<sup>35,36</sup>  
30 have also been employed. While the peristaltic pump and solenoid mini-pump  
31 propel solutions forward, syringe pump operation comprises two alternating  
32 steps, one for solution loading and another for solution delivery. This working  
33 pattern has a potential limiting factor, but may be overcome by including  
34 solenoid valves in the manifold.<sup>35-37</sup> Syringe pumps have a relatively simple  
35 design that enables their construction without the need of sophisticated  
36 machining of components, thus making them cost-effective fluid propelling  
37 devices that can be constructed in a typical laboratory workshop.

38  
39 In the present work, we have developed a multicommuted flow system  
40 for the simultaneous determination of sulfate and chloride in MIC digests of  
41  
42  
43  
44  
45  
46  
47  
48  
49  
50  
51  
52  
53  
54  
55  
56  
57  
58  
59  
60

1  
2  
3 petroleum coke. The flow analysis setup was designed to use a homemade  
4 syringe pump as the fluid propelling device.  
5

6 Usually, the manifold base on the multisyringe approach has been  
7 designed to allow a sample aliquot to be inserted into a holding coil, which is  
8 subsequently displaced toward the detector by reverting the direction of the  
9 syringe piston displacement. The addition of reagent solutions to the sample  
10 zone is performed while the second step proceeds.<sup>35,36,38,39</sup> This configuration  
11 has been successfully employed for the determination of individual analytes.  
12 Intending to develop a procedure for the simultaneous determination of sulfate  
13 and chloride in MIC digests of coke samples, a flow system based on  
14 multicommutated flow analysis process,<sup>40,41</sup> was designed with two sampling  
15 loops instead of a holding coil. Control software was designed to perform the  
16 displacement of the syringe pistons, thus controlling the commutation of  
17 solenoid valves in order to load sampling loops with slugs of sample and  
18 reagents solution for each analyte. This arrangement allowed that reactions to  
19 produce the chemical species to be detected, begin while the sampling step  
20 proceeded, thus improving the sampling rate.  
21  
22  
23  
24  
25  
26  
27  
28  
29  
30  
31

## 32 **2. Experimental**

### 33 *2.1. Apparatus and accessories*

34  
35  
36  
37 The flow system module and the photometric detector comprised the  
38 following equipment setups and accessories: a motorized homemade syringe  
39 pump furnished with four 5.0 mL glass syringes, four three-way solenoid valves  
40 (HP225T031, NResearch) and an electronic interface controlled by a  
41 microcomputer; a flow analysis manifold comprising seven solenoid pinch  
42 valves (225P011-11, NResearch), and two polyethylene reactor coils (100 cm x  
43 0.8 mm i.d.); Five-way (2 units) and three-way (5 units) flow line junctions  
44 machined in acrylic; a digital interface comprising two integrated circuits  
45 ULN2803, assembled as shown below; two similar photometers, each  
46 employing a 5 mm high-intensity emission LEDs with a maximum emission  
47 wavelength of 472 nm, two OPT301 photodetectors (Texas Instruments), two  
48 glass flow cells with a 50 mm optical path length (1.2 mm i.d.), molded as  
49 described elsewhere,<sup>42</sup> two BC547 transistors and two variable resistors (5 k $\Omega$ );  
50  
51  
52  
53  
54  
55  
56  
57  
58  
59  
60

1  
2  
3 a stabilized power supply of +12 V and -12 V (0.5 A) to power the photometers,  
4 and a stabilized power supply of 12 V (2.0 A) to feed the syringe pump and  
5 solenoid valves; a microcomputer equipped with a PCL711 electronic interface  
6 card (Advantech) and running a software written in Quick BASIC 4.5.  
7  
8

9  
10 To allow accuracy assessment, an inductively coupled plasma optical  
11 spectrometer (PerkinElmer, Optime 4300 DV, EUA) with an axial view  
12 configuration was used for the determination of S (180.669 nm) and C (193.030  
13 nm) for sulfate analysis, and a modular chromatographic system (Metrohm Ion  
14 Analysis, Herisau, Switzerland), was used for chloride determination.  
15  
16  
17  
18

## 19 20 2.2. Reagents and solutions

21 All solutions were prepared with purified water with an electric  
22 conductivity less than  $0.1 \mu\text{S cm}^{-1}$ . All chemical reagents were of analytical  
23 grade.  
24  
25

26 A  $8.5 \times 10^{-3} \text{ mmol L}^{-1} \text{ NH}_4\text{OH}$  solution (Merk, Darmstadt, Germany) was  
27 prepared by diluting the concentrated reagent in water. A sulfate stock solution  
28 ( $1.000 \text{ g L}^{-1}$ ) was prepared by dissolving  $(\text{NH}_4)_2\text{SO}_4$  (Merk) in water. Working  
29 standard solutions ranging from 10.0 to 700.0  $\text{mg L}^{-1}$  of  $\text{SO}_4^{2-}$  were prepared by  
30 appropriate dilution of the stock solution with  $50 \text{ mmol L}^{-1} \text{ NH}_4\text{OH}$ . A 10% (w/v)  
31  $\text{BaCl}_2 \cdot 2\text{H}_2\text{O}$  solution (Merck) was prepared by dissolving the respective solid in  
32 a 0.1% (w/v) Tween 80 solution (Merck). A 0.4% (w/v) EDTA solution (Merck)  
33 was prepared by dissolving the solid in a  $0.2 \text{ mol L}^{-1} \text{ NaOH}$  solution (Merck).  
34  
35  
36  
37  
38

39 The chloride stock solution ( $1.000 \text{ g L}^{-1}$ ) was prepared by dissolving  
40 NaCl in water. Working standard solutions ranging from 0.06 to 10.00  $\text{mg L}^{-1}$  of  
41  $\text{Cl}^-$ , were prepared by dilution of the stock solution with  $50 \text{ mmol L}^{-1} \text{ NH}_4\text{OH}$ . A  
42 0.06% (w/v)  $\text{Hg}(\text{SCN})_2$  (Merck) plus 1% (w/v)  $\text{Fe}(\text{NO}_3)_3 \cdot 9\text{H}_2\text{O}$  (Merck) solution  
43 was prepared by dissolving the mercury compound in 15 mL absolute ethanol  
44 (Merck). A 1% (w/v)  $\text{Fe}(\text{NO}_3)_3 \cdot 9\text{H}_2\text{O}$  solution was prepared by dissolving 1.000  
45 g of solid in 4 mL of a  $5 \text{ mol L}^{-1} \text{ HNO}_3$  solution. After dissolution, this was added  
46 to the mercury solution and the volume was made up to 100 mL with water.  
47  
48  
49  
50  
51  
52

## 53 54 2.3. Sample preparation

55 The petroleum coke samples were decomposed employing the  
56 microwave induced combustion (MIC) methodology,<sup>6</sup> using a microwave oven  
57  
58  
59  
60

(Multiwave 3000, Anton Paar, Graz, Austria) equipped with 8 quartz vessels (80 mL, maximum temperature and pressure of 280 °C and 80 bar, respectively). After cryogenic milling and drying to constant mass, samples were pressed as pellets using a hydraulic press (15 ton, Specac, Orpington, UK) prior to MIC decomposition. Sample pellets (500 mg) were positioned in a quartz holder containing a disc of filter paper wetted with 50  $\mu\text{L}$  of a 6 mol L<sup>-1</sup> NH<sub>4</sub>NO<sub>3</sub> (Merck), used as the igniter for MIC. The holder was positioned into a quartz tube with 6 mL of 50 mmol L<sup>-1</sup> NH<sub>4</sub>OH (Merck), used as the absorbing solution to retain Cl and S compounds after combustion. Each vessel was pressurized with 20 bar of oxygen (99.6%, White Martins-Praxair, Brazil) before microwave heating at 1400 W for 5 min (1 min for sample combustion plus 4 min as a reflux step), followed by a cooling step (20 min). After the digestion procedure, all digests were diluted with water to 50 mL for further analyte determination.

The accuracy of the MIC digestion procedure was evaluated by using certified reference material (CRM). Sulfate was determined in a CRM of petroleum coke (NIST 2718, Green Petroleum Coke, National Institute of Standards & Technology, USA), while chloride was determined in a CRM of coking coal (BCR 181, Coking Coal, Institute for Reference Materials and Measurements, Belgium).

#### 2.4. Photometer description

The diagram of the photometers is shown in Fig. 1, and shows that the photometers were designed to be identical, but with independent working conditions. The intensity of the radiation emitted by LED<sub>1</sub> and LED<sub>2</sub> is a function of the electric current intensity flowing through them, controlled by the variable resistors (5 k $\Omega$ ) coupled to the bases of the transistors (Tr<sub>1</sub> and Tr<sub>2</sub>). The radiation beams I<sub>1</sub> and I<sub>3</sub> emitted by LED<sub>1</sub> and LED<sub>2</sub> propagate through the flow cells fc<sub>1</sub> and fc<sub>2</sub>, respectively.

The radiation beams I<sub>2</sub> and I<sub>4</sub> are directed by the glass cylinders (gl) towards the photodetectors Det<sub>1</sub> and Det<sub>2</sub>, respectively, generating electric potential differences (mV) directly related to the intensity of the respective radiation beam. When a flow cell is filled with a solution that absorbs radiation in the same wavelength range as that emitted by the LED, absorption occurs during the propagation of the radiation through the flow cell, causing an

attenuation of the radiation beam intensity. As a result, the radiation beams ( $I_2$  and  $I_4$ ) reaching the detectors is less intense ( $I_1 > I_2$  and  $I_3 > I_4$ ).

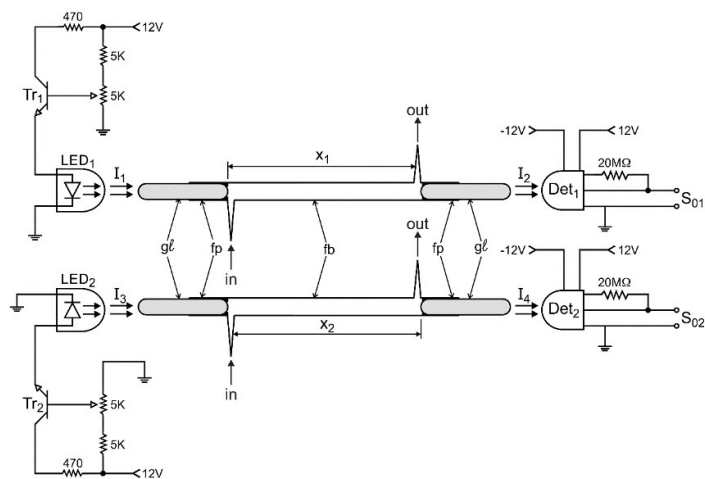


**Figure 1. Diagram of the photometers.**  $Tr_1$  and  $Tr_2$  = transistor BC547;  $LED_1$  and  $LED_2$  = light emitting diode,  $\lambda = 472$  nm; fb = flow cell body, glass tube (boron-silicate);  $x_1$  e  $x_2$  = 50 mm long and 1.2 mm internal diameter; gl = glass cylinders; fp = fused point;  $I_1$ ,  $I_2$ ,  $I_3$ , and  $I_4$  = radiation beams emitted by the LEDs entering and exiting the flow cell, respectively;  $Det_1$  and  $Det_2$  = photodetector OPT301; in and out = fluid input and output, respectively;  $S_{01}$  and  $S_{02}$  = signal generated by the photometers (mV).

The variation of intensity is a function of the concentrations of chemical species in the flow cells. Under these conditions, the electric potential difference generated by each photometer is lower than that when the flow cell is filled with water. This phenomenon was exploited to obtain absorbance values for use in the determination of analyte concentrations.

### 2.5. Description of reactions and flow analysis module

The procedure for chloride determination is based on the displacement reaction of thiocyanate from mercury/thiocyanate compound by chloride ions, followed by the reaction of the liberated thiocyanate with iron(III), forming a colored complex which may be monitored by spectrophotometry.<sup>38,39</sup> The maximum of the absorption band can vary from 460 to 490 nm, depending on the reacting medium.<sup>43</sup> In the current work, the photometric detection was



performed using a blue LED with a maximum emission at 472 nm and a bandwidth of 25 nm.

The procedure for sulfate determination is based on its reaction with barium ions to form a suspension,<sup>23</sup> which causes light scattering in the flow cell, thus decreasing the intensity of the radiation beam. This effect is exploited in the current work with analytical proposal. Over time, accumulation of the barium sulfate precipitate in the flow cell can cause baseline drift. This drawback has been overcome by implementing a cleaning step using an alkaline EDTA solution to dissolve the barium sulfate precipitate,<sup>23</sup> deployed using the flow system manifold shown in Fig. 2.

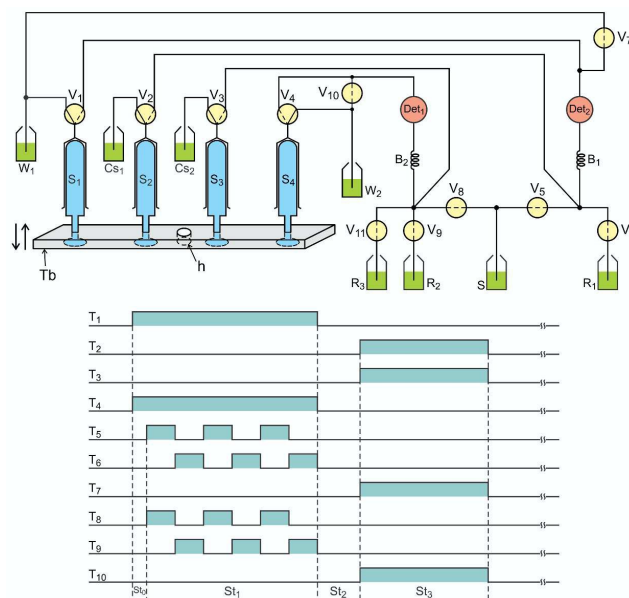


**Figure 2. Diagram of the flow system manifold.** Tb = traction plate of aluminum, h = threaded hole (female) to attach the displacing screw (not shown); S<sub>1</sub>, S<sub>2</sub>, S<sub>3</sub> and S<sub>4</sub> = syringes; V<sub>1</sub>, V<sub>2</sub>, V<sub>3</sub> and V<sub>4</sub> = three way solenoid valve; V<sub>5</sub>, V<sub>6</sub>,...V<sub>11</sub> = pinch solenoid valves; S = sample; R<sub>1</sub> = mercuric thiocyanate solution; R<sub>2</sub> = barium chloride solution; R<sub>3</sub> = EDTA solution; Cs<sub>1</sub>, Cs<sub>2</sub> = carrier solutions ( nitric acid 0.014 mol L<sup>-1</sup> and water respectively; B<sub>1</sub>, B<sub>2</sub> = reaction coil, 100 cm long and 0.8 mm inner diameter; Det<sub>1</sub>, Det<sub>2</sub> = photometer,  $\lambda$  = 472 nm; W<sub>1</sub>, W<sub>2</sub> = waste; T<sub>1</sub>, T<sub>2</sub>, ... T<sub>10</sub> = drive the timing diagram valves V<sub>1</sub>, V<sub>2</sub>, ...V<sub>10</sub>, respectively. Dashed and solid lines in the valve symbols V<sub>1</sub>, V<sub>2</sub>, V<sub>3</sub> and V<sub>4</sub> indicated the fluid pathway when the valves were switched on or off, respectively. Dashed lines in the valve symbols V<sub>5</sub>, V<sub>6</sub> ... V<sub>11</sub> indicate that are normally closed, therefore permit fluid flow only when they are connected.

The flow system setup depicted in Fig. 2 is designed to use an automatic syringe pump for fluid propulsion. The displacement of the syringe pistons forward and backward is performed using the direct current motor of the syringe module, which is coupled to the traction plate (Tb, Fig. 2) using a screw attached to motor shaft.

The section of the manifold comprising syringes S<sub>3</sub> and S<sub>4</sub>, solenoid valves V<sub>3</sub>, V<sub>4</sub>, V<sub>9</sub>, V<sub>10</sub>, and V<sub>11</sub>, reaction coil B<sub>1</sub>, and Det<sub>2</sub> is designed to process the sample for sulfate determination. The section comprising the other devices is for chloride determination.

The interfaces used to drive the syringe pump and the solenoid valves are shown in Fig. 3.

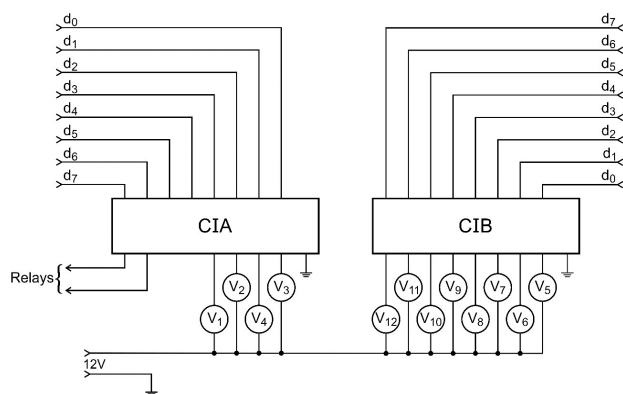


**Figure 3. Diagram of the control interface.** CIA and CIB = integrate circuit ULN2803; V<sub>1</sub>, V<sub>2</sub>, V<sub>3</sub> and V<sub>4</sub> = three-way solenoid valves; V<sub>5</sub>, V<sub>6</sub>, ....., V<sub>12</sub> = solenoid pinch valves normally closed, d<sub>0</sub>, d<sub>1</sub>, .....,d<sub>7</sub> = control lines from the PCL 711 interface card.

The section assigned as CIA is used to drive the syringe motor and solenoid valves V<sub>1</sub>, V<sub>2</sub>, V<sub>3</sub>, and V<sub>4</sub>, which are used to load the syringes with solutions and to direct them toward the flow system. The section assigned as CIB is used to drive the solenoid valves V<sub>5</sub> to V<sub>11</sub>, which comprises the flow system manifold depicted in Fig. 2.

In the configuration shown in Fig. 2, the syringes are in the empty position. When the control software is run, the microcomputer recognizes this position, using the PCL711 card to read a signal generated by the syringe pump. Subsequently, the microcomputer sends a control signal (bits d<sub>7</sub>, d<sub>6</sub>)

1  
2  
3 through the PCL711 interface to activate the syringe pump in order to displace  
4 the syringe piston down, maintaining solenoid valves  $V_1$ ,  $V_2$ ,  $V_3$ , and  $V_4$  in the  
5 off position, thus aspirating the solutions to fill each syringe. When the syringe  
6 piston reaches maximum displacement, the pump motor automatically switches  
7 off and a busy signal is generated to be detected by the microcomputer.  
8  
9

10  
11 The solenoid valves  $V_1$ ,  $V_2$ ,  $V_3$ , and  $V_4$  coupled to the syringes are used  
12 to select the way to displace solutions, while moving the syringe pistons either  
13 upward (forward) or downward (backward). These actions are performed by  
14 controlling the direction of rotation (right or left) of the syringe pump motor.  
15  
16

17  
18 The manifold which handles the sample and reagent solutions  
19 comprises the solenoid valves  $V_5$  to  $V_{11}$ , which work as depicted in the time  
20 switching diagram ( $T_1$ ,  $T_2$ , ...  $T_{10}$ ). Prior to a sampling run, the syringe pump  
21 motor is used to displace the syringe pistons down. In the first step ( $st_1$ ), the  
22 solenoid valves  $V_1$  and  $V_4$  are switched on, while valves  $V_5$ ,  $V_6$ ,  $V_8$ , and  $V_9$  are  
23 switched on/off three times. As we can see, valves  $V_5$  and  $V_8$  are switched on at  
24 the same time, followed by a switching on of valves  $V_8$  and  $V_9$ , and so on. This  
25 sequence loads reaction coil  $B_1$  with a string of slugs of the sample solution in  
26 tandem with slugs of the reagent solution  $R_1$ . A similar sequence loads reaction  
27 coil  $B_2$  with slugs of sample and reagent solution  $R_2$ . Subsequently, the pump  
28 motor is activated to displace the syringe piston up. After a delay time of 2.0 s to  
29 stabilize flow rate, valves  $V_2$  and  $V_3$  are switched on. When this happens, the  
30  $CS_1$  and  $CS_2$  solutions flow through valves  $V_2$ ,  $V_3$ ,  $V_7$ , and  $V_{10}$  towards reaction  
31 coils  $B_1$  and  $B_2$ , respectively. In this configuration, the sample zone containing  
32 the reagent for chloride is displaced through the flow cell of the photometer  
33 ( $Det_2$ ), which generates a signal related to chloride concentration.  
34 Simultaneously, a similar situation occurs with the  $CS_2$  stream, allowing the  
35 monitoring of the signal related to sulfate concentration generated by the  
36 photometer ( $Det_1$ ).  
37  
38  
39  
40  
41  
42  
43  
44  
45  
46  
47  
48  
49

50 This set of actions comprises an analytical run, which can be repeated  
51 the number of times established by the control software. At the end of the  
52 number of runs established, a cleaning step is applied to the sulfate manifold  
53 (reaction coil  $B_2$  and flow cell of the photometer  $Det_1$ ) by aspirating an aliquot of  
54 EDTA solution through them. This step is performed by switching on valves  $V_4$   
55 and  $V_{11}$  for a time interval of 5 s. Following this, valves  $V_3$  and  $V_{10}$  are switched  
56  
57  
58  
59  
60

on for 7 s in order to wash the manifold with the carrier solution (Cs<sub>2</sub>). To perform the cleaning step, the syringe module is activated to displace the piston upward. The set of actions described above is depicted in Table 1.

**Table 1.** Sequence of events.

Step	Event	Rotation	V <sub>1</sub>	V <sub>2</sub>	V <sub>3</sub>	V <sub>4</sub>	V <sub>5</sub>	V <sub>6</sub>	V <sub>7</sub>	V <sub>8</sub>	V <sub>9</sub>	V <sub>10</sub>	V <sub>11</sub>	time/s
1	Reagent fill channel	L	1	0	0	1	0	1	0	0	1	0	1	4.0
2	Channels filling	L	0	0	0	0	0	0	0	0	0	0	0	10
3	Washing analytical path	R	0	1	1	0	0	0	1	0	0	1	0	14
4	Photometer calibration	S	0	0	0	0	0	0	0	0	0	0	0	-
5	Cleaning with EDTA	L	0	0	0	1	0	0	0	0	0	0	1	5.0
6	Cleaning with EDTA	R	0	0	1	0	0	0	0	0	0	1	0	7.0
7	Filling flow lines with sample	L	1	0	0	1	1	0	0	1	0	0	0	3.0
8	Washing sample channel	R	0	1	1	0	0	0	1	0	0	1	0	3.0
9	Sampling for chloride <sup>a</sup>	L	1	0	0	0	1	0	0	0	0	0	0	1.0
	Sampling for chloride <sup>a</sup>	L	1	0	0	0	0	1	0	0	0	0	0	0.5
10	Sampling for sulfate <sup>b</sup>	L	0	0	0	1	0	0	0	1	0	0	0	0.5
	Sampling for sulfate <sup>b</sup>	L	0	0	0	1	0	0	0	0	1	0	0	1.0
11	Signals reading chloride/sulfate	R	0	1	1	0	0	0	1	0	0	1	0	6.0

The events labelled as *a* and *b* correspond to the sampling cycles for chloride and sulfate, respectively. L, R, and S in the rotation column = motor rotation direction for left, right and stop, respectively. V<sub>1</sub> – V<sub>11</sub> = solenoid valves as described in Fig. 2. Numbers 0 and 1 indicate that related valve is switched off or on, respectively. The numbers in the last column are the selected time intervals.

When the program is running, the software queries whether a photometer calibration should be performed. If affirmative, the microcomputer sends control signals to the syringe module to displace the syringe pistons upward and to switch on valves V<sub>2</sub>, V<sub>3</sub>, V<sub>7</sub>, and V<sub>10</sub>. When this happens, the Cs<sub>1</sub> and Cs<sub>2</sub> fluids flow through the flow cells of both photometers in order to fill them with the carrier solutions. The signals generated by the photometers termed here as full-scale measurements (Fsm<sub>1</sub>, Fsm<sub>2</sub>) are adjusted to 2000 mV using the variable resistors wired to the base transistors Tr<sub>1</sub> and Tr<sub>2</sub> (Fig. 1). Afterwards, measurements related to diffuse radiation (Dfm<sub>1</sub> and Dfm<sub>2</sub>) are achieved by aspirating a highly colored solution through both flow cells. These solutions are prepared by mixing 15 mL of a 4% (w/v) SCN<sup>-</sup> solution with equal volumes of standard Fe(III) solutions with concentrations of 40 and 50 mg L<sup>-1</sup>,

1  
2  
3 respectively. The measurements  $D_{fm_1}$  and  $F_{sm_1}$ , and  $D_{fm_2}$  and  $F_{sm_2}$ , related to  
4 the  $Det_1$  and  $Det_2$  photometers, are saved to be used in absorbance  
5 calculations.  
6  
7

8 The calibration step to adjust the full-scale measurements is performed  
9 15 min after powering on the photometer, while assays to achieve diffuse  
10 measurements are performed once a week, since maintaining the full scale  
11 measurements at 2000 mV does not significantly affect their variation. The  
12 steps from 5 to 8 are carried out once prior to beginning the analysis of a new  
13 sample.  
14  
15  
16  
17

18 The calibration step to adjust the full-scale measurements is performed  
19 15 min after powering on the photometer, while assays to achieve diffuse  
20 measurements are performed once a week, since maintaining the full scale  
21 measurements at 2000 mV does not significantly affect their variation. The  
22 steps from 5 to 8 are carried out once prior to beginning the analysis of a new  
23 sample.  
24  
25  
26  
27

28 This flow system was designed to handle sample and reagent solutions  
29 based on the multicommutated process. Therefore, the volumes of sample and  
30 reagent solutions inserted into the manifold are a function of the pumping flow  
31 rate and the time for which the selected valve is switched on. Because the  
32 pumping flow rate was constant throughout, the time intervals and concentration  
33 of the reagent solutions were the variables studied.  
34  
35  
36  
37  
38  
39  
40

### 41 **3. Results and discussion**

#### 42 *3.1. General comments*

43  
44 The method for the photometric determination of chloride based on the  
45 displacement reaction of thiocyanate from mercury/thiocyanate compound by  
46 chloride ions was proposed in the 50's, and has become an alternative to  
47 classical methods, such as the Vollhard and Mohr methods.<sup>43</sup> This method has  
48 a high sensitivity and fast reaction time, allowing the design of high-throughput  
49 flow systems for chloride determination. Furthermore, there is no interference  
50 from other chemical species, so it has become the preferred method for chloride  
51 determination by spectrophotometry.<sup>24,25,31,38,39</sup> On a smaller scale, procedures  
52  
53  
54  
55  
56  
57  
58  
59  
60

1  
2  
3 for the determination of chloride have been proposed based on reaction with  
4 silver nitrate to form a precipitate that may be detected by turbidimetry,<sup>45,46</sup> or by  
5 reaction with silver chloranilate, allowing detection by spectrophotometry.<sup>47,48</sup> In  
6 the former case, the procedure has low sensitivity and low sampling rate. In the  
7 latter, a column filled with solid silver chloranilate ( $\text{Ag}_2\text{Ch}$ ) is coupled to the flow  
8 system manifold, and interference caused by concomitant chemical species is  
9 eliminated by means of an ion exchange resin column attached in tandem with  
10 the silver chloranilate column. However, this requirement is difficult to  
11 implement in a flow system for simultaneous determination. For these reasons,  
12 the method based on reaction with  $\text{Hg}^{2+}$  was selected. The flow system manifold  
13 was designed to work with a reduced volume of reagent, as suggested by AGC  
14 guidelines.<sup>26,27</sup>

### 25 *3.2. Evaluation of the MIC procedure for $\text{Cl}^-$ and $\text{SO}_4^{2-}$ determination* 26 *using MCFA*

27  
28 Digestion efficiency is a critical parameter in analyses performed by the  
29 FIA system. A great deal of interference can be observed if a high amount of  
30 dissolved organic carbon is still present in the final digests. Thus, digestion  
31 efficiency was evaluated by carbon determination using ICP OES. The results  
32 obtained were expressed as RCC, which was always lower than 1% ( $< 5 \text{ mg L}^{-1}$ )  
33 when petroleum coke was digested by MIC. This indicates a high digestion  
34 efficiency, and ensures a determination step almost completely free from  
35 interference due to the presence of carbon in the final digests.

36  
37 The proposed determination system is also dependent on the analyte  
38 species present in the absorbing solution obtained from MIC. For this reason,  
39 we evaluated the oxidation state of the analyte present in the final solution, as it  
40 could negatively impact the detection based on reactions of  $\text{Cl}^-$  and  $\text{SO}_4^{2-}$ . First,  
41 the presence of Cl and S species were determined employing ion exchange  
42 chromatography, the results of which are shown in Fig. 4.

43  
44 Analyzing the read-out displayed in Fig. 4, we observe that only signals  
45 related to the retention times of  $\text{Cl}^-$  and  $\text{SO}_4^{2-}$  are recorded. Species in other  
46 oxidation states, such as  $\text{ClO}_3^-$  and  $\text{SO}_3^{2-}$ , that might cause interference during  
47 the detection step, were not observed in the chromatogram. Therefore, samples  
48  
49  
50  
51  
52  
53  
54  
55  
56  
57  
58  
59  
60

prepared using MIC were considered suitable for further analysis employing the proposed MCFA procedures.

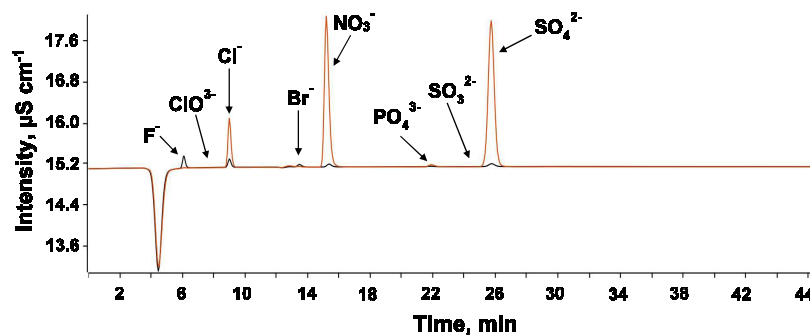


**Figure 4. Chromatogram record of a coke sample after digestion by MIC.** Black line represents the retention time obtained from standard solution. Red line represents the retention time obtained from sample after MIC digestion.

### 3.3. Parameters for sulfate determination

#### 3.3.1. Effects of the sample zone volume

Because the volume of the sample zone can affect the sensitivity of the procedure, assays were performed in order to find the optimal volume. Assays were performed using time intervals of 0.5 and 1.0 s for the sample and barium chloride solution, respectively, and varying the number of sampling cycles (Table 1). These experiments yielded the results shown in Fig. 5. These results show that the signal increases with the volume of the sample zone up to 2100  $\mu\text{L}$ , while for a volume of 2400  $\mu\text{L}$  no significant increase in the signal is observed. This effect is normal for a flow system. The volume of the sample zone can be selected within this volume range in order to achieve the required analytical result. However, it is important to consider that a large sample volume can improve sensitivity, but will impair the sampling throughput.

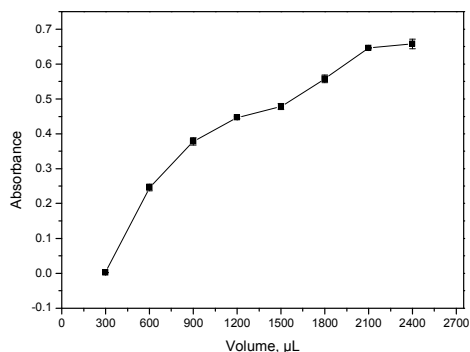


**Figure 5. Effect of the sample zone volume.** Assay carried out using a  $50 \text{ mgL}^{-1}$  sulphate and flow rate of  $200 \mu\text{Ls}^{-1}$ .

### 3.3.2. Effect of reagent volume

With the reagent concentration being kept constant, the optimum amount available for the reaction was investigated as a function of the volume inserted while performing the sampling step. In order to find the optimum signal response, we experimented with keeping the solenoid valve  $V_9$  on for time intervals of 0.25, 0.5, 1.0, 1.5, and 2.0 s (Fig. 2) and applied five sampling cycles. Under these conditions, the volume of reagent solution per sampling cycle varied from 50 to 400  $\mu\text{L}$ , while the volume of the sample slug was 200  $\mu\text{L}$ . No significant variation in the magnitude of the signals is observed for the time intervals ranging from 0.5 to 1.5 s. However, a decrease in signal magnitude was observed with a time interval of 2.0 s. In this case, there could have been a dispersion effect due to the volume of the reagent solution aliquot, which was twice the volume of the sample aliquot. Considering these results, we selected a time interval of 1.0 s for subsequent evaluations.

### 3.3.3. Photometer response for sulfate determination

The analytical procedure was based on light scattering caused by the barium sulfate suspension produced. Absorbance is generally employed as the parameter to achieve sulfate concentration. Spectrophotometers equipped with an optical system typically emit a radiation beam with a narrow wavelength band, tending to be parallel. However, in the present work we employed a



homemade photometer using an LED as the radiation source, which provided a radiation beam that was neither monochromatic nor parallel. Since these features would impair the range of linear responses, we implemented a set of assays to establish the best absorbance range to be used when using a LED based photometer. The signal generated by the flow system presented a transient signal profile related to analyte concentration, as shown in Fig. 6.

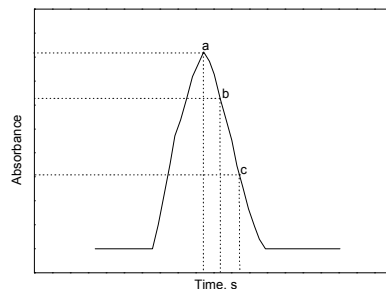


**Figure 6. Record of the transient signal.** Record referred to  $200 \text{ mg L}^{-1}$  sulphate standard solution and settling three sampling cycles. Other parameters as described before.

Usually, the value of the peak height was used as the measurement parameter. Each point on the resultant profiles is associated with an instantaneous analyte concentration. This feature has been exploited previously to perform on-line dilution.<sup>49,50</sup> In the present work, it was used to determine the range where absorbance could be used as the parameter for sulfate determination. Since each point on the signal profile represents an analyte concentration, data acquisition was programmed to use an increased delay time before the signal monitoring began. The evaluations were performed using sulfate standard solutions with concentrations ranging from  $50$  to  $700 \text{ mg L}^{-1}$ . Taking into account the maximum value of the signal as a measurement parameter, and applying a linear regression methodology, we achieved the results shown in Table 2.

The results shown in the first row of Table 2 are related to the measurements carried out without a delay time ( $\Delta t = 0$ ), thus the maximum peak height was achieved by monitoring the whole sample zone. The results, including absorbance range, shown in the second and third rows are similar to that of the first. When the delay times are set at  $6.0$  and  $8.0 \text{ s}$ , the absorbance

range narrows and its magnitude is reduced significantly. This indicates that the signal reading step begins at the falling edge of the signal profile (Fig. 6). Nevertheless, an improvement in linearity is observed. As we can see, similar results are achieved when three sampling cycles are used. In this case, the volume of the sample zone is increased by 50%, which serves to widen the absorbance range, but no improvement in linearity is observed. However, when the delay time is 6.0 and 8.0 s, the absorbance ranges are similar to those observed for two sampling cycles.

The results shown in the first row of Table 2 are related to the measurements carried out without a delay time ( $\Delta t = 0$ ), thus the maximum peak height was achieved by monitoring the whole sample zone.

**Table 2. Photometer response as function of delay time**

Sampling cycles	$\Delta t$ (s)*	Intercept	Slope	R	Absorbance range
2.0	0	0.2083	0.0019	0.9771	0.2421 – 1.4585
	2.0	0.2017	0.0019	0.9772	0.2368 – 1.4349
	4.0	0.1951	0.0019	0.9806	0.2226 – 1.4157
	6.0	0.0590	0.0014	0.9943	0.1024 – 1.0102
	8.0	0.0369	0.0006	0.9983	0.0707 – 0.5235
3.0	0	0.3820	0.0026	0.9609	0.4158 – 1.9890
	2.0	0.3761	0.0026	0.9676	0.4150 – 2.0316
	4.0	0.3680	0.0025	0.9633	0.4037 – 1.8886
	6.0	0.1540	0.0014	0.9933	0.2076 – 1.0927
	8.0	0.0064	0.0008	0.9933	0.0553 – 0.6051

\*Delay time before beginning the signal reading step.

The results, including absorbance range, shown in the second and third rows are similar to that of the first. When the delay times are set at 6.0 and 8.0 s, the absorbance range narrows and its magnitude is reduced significantly. This indicates that the signal reading step begins at the falling edge of the signal profile (Fig. 6). Nevertheless, an improvement in linearity is observed.

1  
2  
3 As we can see, similar results are achieved when three sampling cycles  
4 are used. In this case, the volume of the sample zone is increased by 50%,  
5 which serves to widen the absorbance range, but no improvement in linearity is  
6 observed. However, when the delay time is 6.0 and 8.0 s, the absorbance  
7 ranges are similar to those observed for two sampling cycles.  
8  
9

10  
11 The results shown in Table 2 show that samples within a wide  
12 concentration range can be processed employing a delay time of 6.0 or 8.0 s.  
13 The linear responses achieved for both time intervals are better than those  
14 reported in previous papers.<sup>22,23</sup> Analyzing the linear relationship of the results  
15 shown in Table 2, we observe that an absorbance value of around 1.0 is a  
16 limiting value of the proposed setup, when light scattering by suspension of  
17 particles was associated with the analyte concentration.  
18  
19

20  
21 Based on these results, we decided that the optimum conditions for our  
22 system are: three sampling cycles, time intervals of 0.5 and 1.0 s for the  
23 insertion of sample and reagent solutions, respectively, and a delay time of 6.0  
24 s before beginning the signal reading step. To find the overall response of the  
25 proposed system, a set of sulfate standard solutions at concentrations of 10, 25,  
26 50, 100, 150, 200, 300, 400, 500, 600, and 700 mg L<sup>-1</sup> was processed. The  
27 maximum peak height was chosen as the measuring parameter, giving the  
28 following linear relationship: absorbance = 0.0554 + 0.0013 mg L<sup>-1</sup> C (r =  
29 0.9994). This sulfate concentration range is wider than those presented in  
30 previous papers.<sup>22,23,42</sup> This could be considered as a useful advantage,  
31 allowing analysis of samples with a wide concentration range without any  
32 change in the flow system structure or working pattern.  
33  
34  
35  
36  
37  
38  
39  
40  
41  
42  
43

#### 44 3.3.4 Effect of EDTA as a cleaning solution

45  
46  
47 The barium sulfate suspension tended to adhere to the inner wall of the  
48 reaction coil, causing baseline drift and eventually can clog it. To overcome this  
49 drawback, a cleaning step using an EDTA solution in alkaline medium was  
50 implemented, as described in the experimental section. The assay was  
51 performed using EDTA solutions with concentrations of 0.05, 0.1, 0.2, 0.4, and  
52 0.6% (w/v) prepared in a 0.2 mol L<sup>-1</sup> NaOH solution and an 800 mg L<sup>-1</sup> sulfate  
53 standard solution. When EDTA solutions with concentrations of 0.2, 0.4 and  
54  
55  
56  
57  
58  
59  
60

0.6% (w/v) were pumped through the reaction and flow cell for 5.0 s, no base line drift was observed. Thus, a 0.4% EDTA solution was selected for subsequent evaluations.

### 3.4. Parameters for chloride determination

#### 3.4.1. Effect of sample volume

Considering that the sample volume can affect the magnitude of the analytical signal, we evaluated the appropriate volume to be used. The assay was performed with solenoid valve  $V_1$  switched on (Fig. 2) while the syringe pistons were forced down. At the same time, solenoid valves  $V_5$  and  $V_6$  were switched on/off alternately three-times (three sampling cycles). Valve  $V_6$  was kept switched on for 0.5 s, while the time interval for solenoid valve  $V_5$  was varied from 0.5 to 2.5 s. Under these conditions, the volumes of sample slugs were varied from 100 to 500  $\mu\text{L}$ . The results show an increase of up to 20% when the slug volume increased from 100 to 200  $\mu\text{L}$ . Since identical values for higher volumes were obtained, a time interval of 1.0 s was selected.

#### 3.4.2 Effect of the reagent solution volume

Mercury thiocyanate was prepared as a saturated solution, thus the establishment of the best conditions for the reaction involved the variation of solution volume only. The time intervals for the switching on/off of solenoid valve  $V_2$  (Fig. 2) were varied from 0.13 to 1.00 s, at increments of 0.25 s. The assays were performed using a 10.0 mg  $\text{L}^{-1}$  chloride standard solution and three sampling cycles. With an aspiration flow rate of syringe  $S_1$  at 200  $\mu\text{Ls}^{-1}$ , the volume of the reagent solution slugs was varied between 25 and 200  $\mu\text{L}$ . The results show a small increment in signal when the slug volume increases from 25 to 50  $\mu\text{L}$ , and a tendency for constant values at higher volumes. Based on these results, a time interval of 0.5 s was selected for additional experiments.

### 3.5. Simultaneous determination of sulfate and chloride

The assays discussed above were performed to find the appropriate operational conditions for both analytes. The selected values of the variables studied are summarized in Table 3.

**Table 3. Selected values of the studied variables**

Parameter	Chloride		Sulfate	
	Studied range	Chosen	Studied range	Chosen
Sample insertion time (s)	0.5 – 2.5	1.0	0.25 – 2.0	0.5
Reagent insertion time (s)	0.125 – 1.0	0.5	0.25 – 2.0	1.0
Sampling cycles	2 – 10	3	1 – 5	3

The evaluations previously discussed were carried out individually for each analyte. This section discusses the results achieved when running the flow system (Fig. 2) for simultaneous determination, yielding the results shown in Fig. 7. The uniformity of the results indicates the excellent performance of the proposed setup. The curves shown in Fig. 7a and 7b show that, for both analytes, a wide range of linear responses was achieved.

We compared the performance of our system with other existing analytical procedures for the determination of chloride and sulphate in water samples. Because samples of petroleum coke digested using MIC can be considered similar to a water sample, several papers which measured chloride and sulfate in aqueous samples were selected as references for comparison.<sup>31,38,51,52</sup> The parameters employed to evaluate the features of the analytical procedures used in these works are summarized in Table 4.

Analyzing the results of the proposed procedure in terms of sulfate determination we observe that, overall, they are favorable to the proposed procedure. The reagent consumption is higher than that in Ref. 51, but the linear range of our proposed procedures is wider, which is an advantage for large scale routine analysis.

We compared the performance of our system with other existing analytical procedures for the determination of chloride and sulphate in water samples. Because samples of petroleum coke digested using MIC can be considered similar to a water sample, several papers which measured chloride and sulfate in aqueous samples were selected as references for

comarison.<sup>31,38,51,52</sup> The parameters employed to evaluate the features of the analytical procedures used in these works are summarized in Table 4.

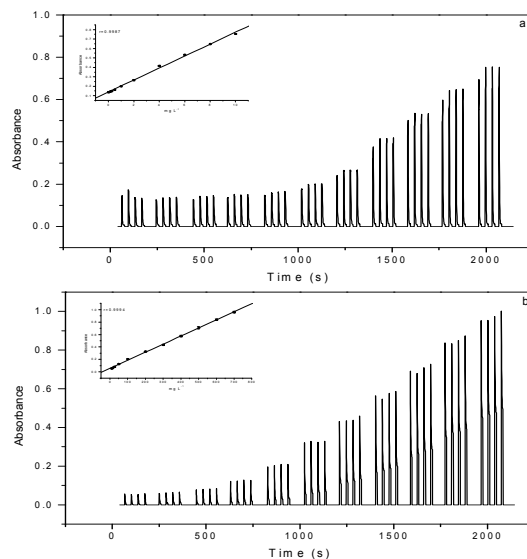


**Figure 7. Records of the transient signals generated simultaneously.** The set of record labeled as *a* correspond to chloride standard solutions of 0.0, 0.06, 0.125, 0.25, 0.5, 1.0, 2.0, 4.0, 6.0, 8.0, 10.0 mg L<sup>-1</sup>, while the other one labelled as *b* is related with sulphate standard solutions of 10, 15, 25, 50, 100, 200, 300, 400, 500, 600, 700 mg L<sup>-1</sup>.

Analyzing the results of the proposed procedure in terms of sulfate determination we observe that, overall, they are favorable to the proposed procedure. The reagent consumption is higher than that in Ref. 51, but the linear range of our proposed procedures is wider, which is an advantage for large scale routine analysis.

The results in terms of chloride determination show that the reagent consumption of the procedure reported in Ref. 30, is lower than that of the proposed procedure, but the volume of waste generated containing mercury is twofold. The others parameters are similar, except for the sampling rate for individual chloride determinations, which is 75 determinations per hour for the proposed procedure. However, an equal number of sulfate determinations are possible.

**Table 4. Performance comparison**

Parameters	Proposed procedure	Ref. 51	Ref. 52	Proposed procedure	Ref. 31	Ref. 38
	(SO <sub>4</sub> <sup>2-</sup> )	(SO <sub>4</sub> <sup>2-</sup> )	(SO <sub>4</sub> <sup>2-</sup> )	(Cl <sup>-</sup> )	(Cl <sup>-</sup> )	(Cl <sup>-</sup> )
Linear range (mg L <sup>-1</sup> )	10 - 700	20 - 200	10- 100	0.25 -10	1 - 10	1 - 40
Linear coef. (r)	0.9986	0.999	0.999	0.9994	0.996	0.999
Detection limit (mg L <sup>-1</sup> )	5.3	3.0	10.0	0.16	0.4	0.2
Reagent consumption (mg L <sup>-1</sup> )	20 <sup>a</sup>	5.0 <sup>a</sup>	22 <sup>a</sup>	0.12 <sup>b</sup>	0.1 <sup>b</sup>	0.05 <sup>b</sup>
Coefficient of variation (%)	3.0	2.4	1.6	0.9	2.3	0.8
Waste (mL) <sup>c</sup>	3.0	6.4	7.8	2.5	3.0	5.9
Sampling rate (h <sup>-1</sup> )	75	30	20	75	50	130

The labels *a* and *b* correspond to the consumption of barium and mercury per determination, respectively, while *c* indicates the volume of waste generated per determination.

### 3.5. Simultaneous determination of sulfate and chloride

In order to verify the effectiveness of the proposed MCFA system for simultaneous determination of sulfate and chloride, we analyzed digested samples of petroleum coke. Under the optimized conditions, six samples of petroleum coke were analyzed. The results obtained are presented in Table 5. For comparison, the samples were also analyzed using IC for chloride and ICP OES for sulfate (as total S). Both results are also presented in Table 5. Applying the paired *t*-test at a 95% confidence level, we obtained values of  $t_{\text{tcal}} = 0.30$  and  $t_{\text{tcal}} = 0.32$  for chloride and sulfate, respectively. The tabulated value for this

confidence level is  $t_{\text{tab}} = 2.57$ , indicating that, for both analytes, there is no significant difference between the results.

**Table 5. Result comparison of chloride and sulfate in petroleum coke.**

Sample	Chloride		Sulfate	
	Proposed procedure mg L <sup>-1</sup>	Reference method (IC) mg L <sup>-1</sup>	Proposed procedure mg L <sup>-1</sup>	Reference method (ICP-OES) mg L <sup>-1</sup>
1	0.345 ± 0.020	0.372 ± 0.024	354.1 ± 2.5	349.5 ± 1.7
2	0.424 ± 0.020	0.462 ± 0.019	341.9 ± 2.0	331.6 ± 2.3
3	0.640 ± 0.070	0.487 ± 0.022	337.6 ± 4.1	336.1 ± 3.7
4	0.425 ± 0.005	0.512 ± 0.013	331.9 ± 4.4	335.6 ± 2.0
5	0.229 ± 0.040	0.402 ± 0.018	338.1 ± 5.0	339.6 ± 0.6
6	0.510 ± 0.050	0.428 ± 0.030	341.1 ± 4.6	346.1 ± 4.4

Results are the average of three consecutive measurements

#### 4. Conclusion

Our proposed MCFA system was used for chloride and sulfate determination in samples of petroleum coke prepared using digestion by MIC methodology. The results of these experiments clearly indicated that the system presents a convenient and efficient method, capable of high sampling throughput and a wide analytical range.

Additionally, the high digestion efficiency obtained using MIC, combined with the possibility of using diluted absorbing solutions, makes reagent coupling an easy and effective method for sulfate and chloride determination, even for samples which are hard to dissolve, such as petroleum coke.

The robustness of the proposed prototype system of syringes pump, and photometers is evinced by the fact that the setup operated for six months without requiring the replacement of a single component. The configuration of the flow system manifold allowed a sampling throughput higher than that usually attained employing a syringe pump as the fluid propelling device.<sup>35,36,39</sup> Furthermore, the effective concentration range of our system was shown to be wider than those reported for methods presented in earlier works.<sup>22,23,31,32</sup>

The proposed setup, and the optimized analytical procedure developed with it, combine favorable features, making our proposed methodology a cost-



effective alternative for sulfate and chloride determination in samples of petroleum coke. Its low volume of waste generation is a particularly useful feature considering the current importance of environmental sustainability.

### Acknowledgements

The authors acknowledge financial support from FAPESP (process 2013/05728-2; 2011/23498-9) CNPq, CAPES, and INCTAA.

### 5. References

- 1 Z. Zhou, Q. Hu, X. Liu, G. Yu, F. Wang, *Energy Fuels*, 2012, **26**, 1489-1495.
- 2 P. Córdoba, O. Font, M. Izquierdo, X. Querol, C. Leiva, M. A. López-Antón, M. Díaz-Somoano, R. Ochoa-González, M. R. Martínez-Tarazonab, P. Gómez, *Fuel*, 2012, **102**, 773-788.
- 3 P. Córdoba, R. Ochoa-Gonzalez, O. Font, M. Izquierdo, X. Querol, C. Leiva, M.A. López-Antón, M. Díaz-Somoano, M. R. Martínez-Tarazona, C. Fernandez, A. Tomás, *Fuel*, 2012, **92**, 145-157.
- 4 L. F. O. Silva, M. L. S. Oliveira, C. H. Sampaio, I. A. S. Brum, J. C. Hower, *Energy Fuels*, 2013, **27**, 1194-1203.
- 5 M. A. Duchesnea, A. Y. Ilyushechkin, R. W. Hughes, D. Y. Lu, D. J. McCalden, A. Macchi, E. J. Anthony, *Fuel*, 2012, **97**, 321-328.
- 6 J. S. F. Pereira, P. A. Mello, D. P. Moraes, F. A. Duarte, V. L. Dressler, G. Knapp, E. M. M. Flores, *Spectrochim. Acta Part B*, 2009, **64**, 554-558.
- 7 B. Fernández, J. M. Almanza, J. L. Rodríguez, D. A. Cortes, J. C. Escobedo, E. J. Gutiérrez, *Ceram. Int.*, 2011, **37**, 2973-2979.
- 8 J. Chen, X. Lu, *Resour. Conserv. Recycl.*, 2007, **49**, 203-2016.
- 9 F. G. Antes, M. F. P. Santos, R. C. L. Guimarães, J. N. G. Paniz, E. M. M. Flores, V. L. Dressler, *Anal. Methods*, 2011, **3**, 288-293.
- 10 A. I. Lugovskoi, S. A. Loginov, G. G. Musienko, F. M. Khutoryanskii, L. N. Orlov, A. G. Mikhalev, *Chem.Tech Fuels and Oils*, 2000, 36, No 5.
- 11 J.S.F. Pereira, L.O. Diehl, F.A. Duarte, M.F.P. Santos, R.C.L. Guimarães, V.L. Dressler, E.M.M. Flores, *J. Chromatogr. A*, 2008, **1213**, 249-252.

- 1  
2  
3 12 J. Aramendia, L. Gómez-Nubla, K. Castro, J. M. Madariaga, *Microchem. J.*,  
4 2014, **115**, 138-145.  
5  
6 13 J. Aramendia, L. Gomez-Nubla, I. Arrizabalaga, N. Prieto-Taboada, K.  
7 Castro, J. M. Madariaga, *Corros. Sci.*, 2013, **76**, 154-162.  
8  
9 14 A. Demirak, A. Balci, H. Karaoglu, B. Tosmur, *Environmental Monitoring and*  
10 *Assessment*, 2006, **123**, 271–283.  
11  
12 15 C. M. González, B. H. Aristizábal, *Atmospheric Environment*, 2012, **60**, 164-  
13 171.  
14  
15 16 P. Córdoba, O. Font, M. Izquierdo, X. Querol, C. Leiva, M. A. López-Antón,  
16 M. Díaz-Somoano, R. Ochoa-González, M.R. Martinez-Tarazona, P. Gómez,  
17 *Fuel*, 2012, **102** 773-788.  
18  
19 17 Annual Book of ASTM Standards. ASTM standard D 5016-03, Standard Test  
20 Method for Sulphur in Ash from Coal, Coke, and Residues from Coal  
21 Combustion Using High-Temperature Tube Furnace Combustion Method with  
22 Infrared Absorption.  
23  
24 18 J. A. Vieira, I. M. Raimundo, B. F. Reis, *Anal. Chim. Acta* 2001, **438**, 75–81.  
25  
26 19 E. Piccin, H. J. Vieira, O. Fatibello-Filho, *Anal. Lett.*, 2005, **38**, 511–522.  
27  
28 20 F. V. Silva, A. R. A. Nogueira, G. B. Souza, E. A. G. Zagatto, *Anal. Chim.*  
29 *Acta*, 1998, **370**, 39-46.  
30  
31 21 E. R. Alves, P. R. Fortes, E. P. Borges, E. A. G. Zagatto, *Anal. Chim. Acta*,  
32 2006, **564**, 231-235.  
33  
34 22 S. M. B. Brienza, R. P. Sartini, J. A. Gomes Neto, E. A. G. Zagatto, *Anal.*  
35 *Chim. Acta*, 1995, **308**, 269-274.  
36  
37 23 F. J. Krug, E. A. G. Zagatto, B. F. Reis, O. Bahia F<sup>o</sup>, A. O. Jacintho, *Anal.*  
38 *Chim. Acta*, 1983, **145**, 179-187.  
39  
40 24 F. A. Duarte, E. R. Pereira, E. L. M. Flores, E. I. Muller, E. M. M. Flores, V. L.  
41 Dressler, *Quim. Nova*, 2013, **36**, 716-719.  
42  
43 25 C. R. Silva, H. J. Vieira, L. S. Canaes, J. A. Nóbrega, O. Fatibello-Filho,  
44 *Talanta*, 2005, **65**, 965-970.  
45  
46 26 S. Armenta, S. Garrigues, M. de la Guardia, *Anal. Chem.* 2008, **27**, 497-511.  
47  
48 27 W. R. Melchert, F. R. P. Rocha, B. F. Reis, *Anal. Chim. Acta*, 2012, **714**, 8-  
49 19.  
50  
51 28 F. R. P. Rocha, B. F. Reis, E. A. G. Zagatto, J. L. F. C. Lima, R. A. S. Lapa,  
52 J. L. M. Santos, *Anal. Chim. Acta*, 2002, **468**, 119-131.  
53  
54  
55  
56  
57  
58  
59  
60

- 1  
2  
3 29 A. F. Lavorante, M. A. Feres, B. F. Reis, *Spectrosc. Lett.*, 2006, **39**, 631–  
4 650.  
5  
6 30 M. A. Feres, B. F. Reis, *Talanta*, 2005, **68**, 422-428.  
7  
8 31 F. R.P. Rocha, Patrícia B. Martelli, B. F. Rei, *Anal. Chim. Acta*, 2001, 438,  
9 11–19.  
10  
11 32 R. C. Prados-Rosales, J. L. Luque-García, M. D. Luque de Castro, *Anal.*  
12 *Chim. Acta*, 2002, **461**, 169-180.  
13  
14 33 W. R. Melchert, F. R. P. Rocha, *Anal. Chim. Acta*, 2008, **616**, 56-62.  
15  
16 34 S. S. M. Rodrigues, J. L. M. Santos, *Talanta*, 2012, **96**, 210-215.  
17  
18 35 L. Chaparro, L.Ferrer, L. Leal, V. Cerdà, *Talanta* 2015, **133**, 94–99.  
19  
20 36 F. Maya, J. M. Estela, V. Cerdà, *Talanta*, 2011, **85**, 588–595.  
21  
22 37 G. P. Vieira, S. R. W. Perdigão, M. F. Fiore, B. F. Reis, *Sens. Actuators B*,  
23 2012, **161**, 422-428.  
24  
25 38 V. Cerdà, R. Forteza, J. M. Estela, *Anal. Chim. Acta*, 2007, **600**, 35–45.  
26  
27 39 F. Maya, J. M. Estela, V. Cerdà, *Anal. Bioanal. Chem.* 2009, **394**,1577–  
28 1583.  
29  
30 40 T. R. Dias, J. J. R. Rohwedder, M. A. S. Brasil, B. F. Reis, *Anal. Methods*,  
31 2014, **6**, 9667–9674.  
32  
33 41 G. P. Vieira, C. C. Crispino, S. R. W. Perdigão, B. F. Reis, *Anal. Methods*,  
34 2013, **5**, 489–495.  
35  
36 42 T. R. Dias, M. A. S. Brasil, M. A. Feres, B. F. Reis, *Sens. Actuators B*, 2014,  
37 **198**, 428-454.  
38  
39 43 D.M. Zall, D. Fisher, M. Q. Garner, *Anal. Chem.* 1956, **28**, 1655-1668.  
40  
41 44 F. Maya, J. M. Estela, V. Cerda, *Talanta* 2008 , **74**, 1534–1538.  
42  
43 45 P. R. Fortes, M. A. Feres, E. A.G. Zagatto, *Talanta* 2008, **77**, 571–575  
44  
45 46 I. C. Santos, R. B. R. Mesquita, A. C. Galvis-Sánchez, I. Delgadillo, A. O. S.  
46 S. Rangel, *Food Anal. Water Research* 37 (2003) 4243–4249 2012, **5**, 287–  
47 295.  
48  
49 47 F. Sagara, T. Tsuji, I. Yoshida, D. Ishii, K. Ueno, *Anal. Chim. Acta*, 1992,  
50 **270**, 217-221.  
51  
52 48 V. G. Bonifácio, L. C. Figueiredo-Filho, L. H. Marcolino Jr., O. Fatibello-Filho,  
53 *Talanta* 2007, **72**,663–667.  
54  
55 49 B. F. Reis, A. O. Jacintho, J. Mortatti, F. J. Krug, E. A. G. Zagatto, H.  
56 Bergamin, L. C. R. Pessenda, *Analytica Chimica Acta*, 1981, **123**, 221-228.  
57  
58  
59  
60

1  
2  
3 50 F. G. Santos, B. F. Reis, J. Braz. Chem. Soc., 2013, **24**, 983-990.

4 51 W. R. Melchert, F. R. P. Rocha, Anal. Chim. Acta, 2008, **61**, 656–62.

5  
6 52 I. P. A. Morais, M. R. S. Souto, T. I.M.S. Lopes, A. O. S. S. Rangel, Water  
7 Research, 2003, **37**, 4243–4249.  
8  
9

10  
11  
12  
13  
14  
15  
16  
17  
18  
19  
20  
21  
22  
23  
24  
25  
26  
27  
28  
29  
30  
31  
32  
33  
34  
35  
36  
37  
38  
39  
40  
41  
42  
43  
44  
45  
46  
47  
48  
49  
50  
51  
52  
53  
54  
55  
56  
57  
58  
59  
60

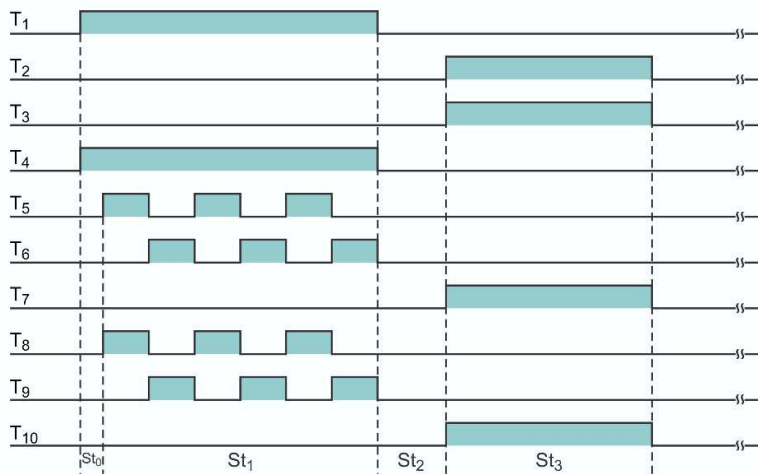
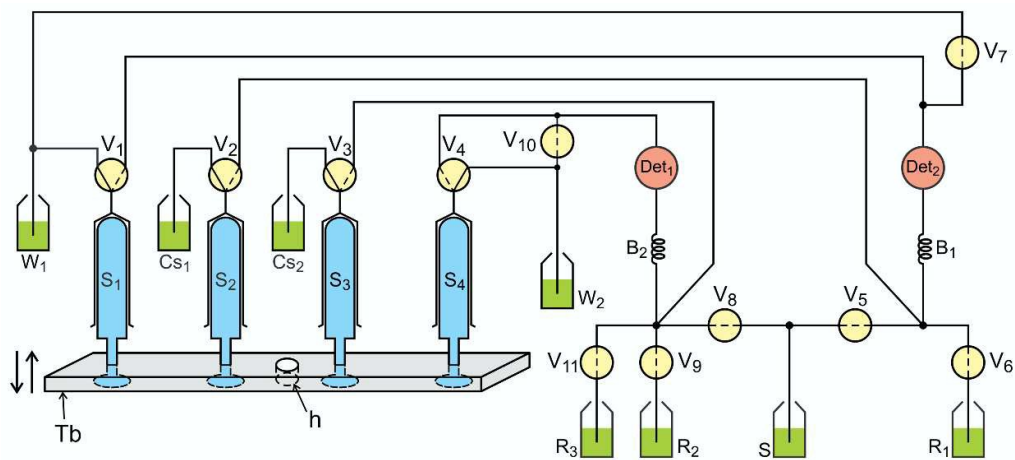
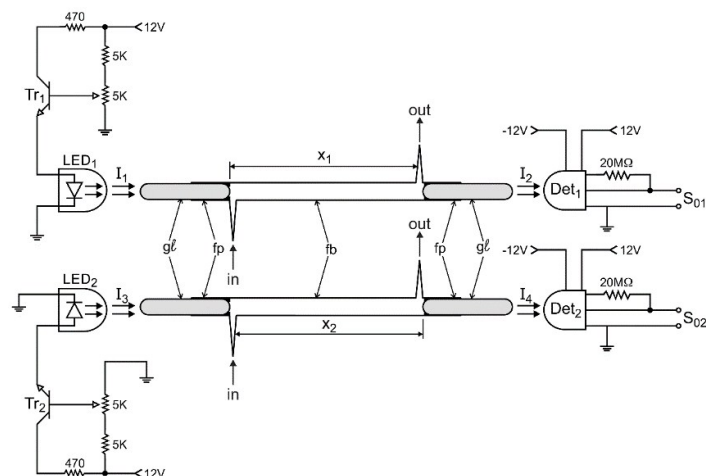


Diagram of the flow system and its working pattern

1  
2  
3  
4  
5  
6  
7  
8  
9  
10  
11  
12  
13  
14  
15  
16  
17  
18  
19  
20  
21  
22  
23  
24  
25  
26  
27  
28  
29  
30  
31  
32  
33  
34  
35  
36  
37  
38  
39  
40  
41  
42  
43  
44  
45  
46  
47  
48  
49  
50  
51  
52  
53  
54  
55  
56  
57  
58  
59  
60



**Figure 1. Diagram of the photometers.**  $Tr_1$  and  $Tr_2$  = transistor BC547;  $LED_1$  and  $LED_2$  = light emitting diode,  $\lambda = 472$  nm; fb = flow cell body, glass tube (boron-silicate);  $x_1$  e  $x_2$  = 50 mm long and 1.2 mm internal diameter; gl = glass cylinders; fp = fused point;  $I_1$ ,  $I_2$ ,  $I_3$ , and  $I_4$  = radiation beams emitted by the LEDs entering and exiting the flow cell, respectively;  $Det_1$  and  $Det_2$  = photodetector OPT301; in and out = fluid input and output, respectively;  $S_{01}$  and  $S_{02}$  = signal generated by the photometers (mV).

 1  
2  
3  
4  
5  
6  
7  
8  
9  
10  
11  
12  
13  
14  
15  
16  
17  
18  
19  
20  
21  
22  
23  
24  
25  
26  
27  
28  
29  
30  
31  
32  
33  
34  
35  
36  
37  
38  
39  
40  
41  
42  
43  
44  
45  
46  
47  
48  
49  
50  
51  
52  
53  
54  
55  
56  
57  
58  
59  
60

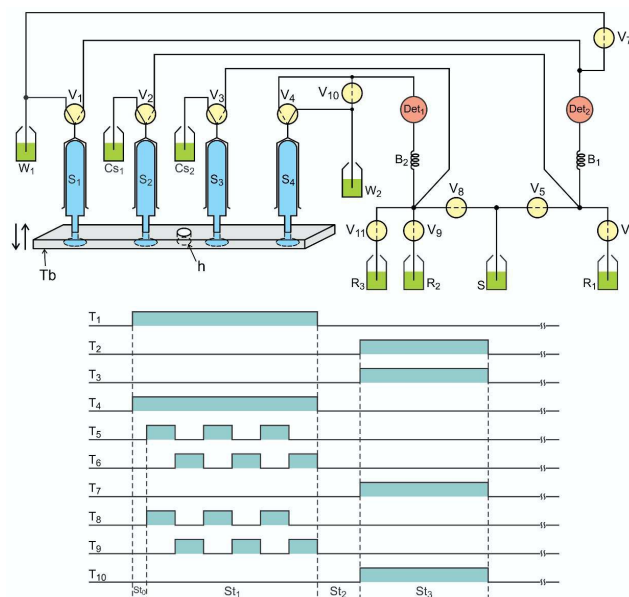


**Figure 2. Diagram of the flow system manifold.** Tb = traction plate of aluminum, h = threaded hole (female) to attach the displacing screw (not shown); S<sub>1</sub>, S<sub>2</sub>, S<sub>3</sub> and S<sub>4</sub> = syringes; V<sub>1</sub>, V<sub>2</sub>, V<sub>3</sub> and V<sub>4</sub> = three way solenoid valve; V<sub>5</sub>, V<sub>6</sub>,...V<sub>11</sub> = pinch solenoid valves; S = sample; R<sub>1</sub> = mercuric thiocyanate solution; R<sub>2</sub> = barium chloride solution; R<sub>3</sub> = EDTA solution; Cs<sub>1</sub>, Cs<sub>2</sub> = carrier solutions ( nitric acid 0.014 mol L<sup>-1</sup> and water respectively; B<sub>1</sub>, B<sub>2</sub> = reaction coil, 100 cm long and 0.8 mm inner diameter; Det<sub>1</sub>, Det<sub>2</sub> = photometer, λ = 472 nm; W<sub>1</sub>, W<sub>2</sub> = waste; T<sub>1</sub>, T<sub>2</sub>, ... T<sub>10</sub> = drive the timing diagram valves V<sub>1</sub>, V<sub>2</sub>, ...V<sub>10</sub>, respectively. Dashed and solid lines in the valve symbols V<sub>1</sub>, V<sub>2</sub>, V<sub>3</sub> and V<sub>4</sub> indicated the fluid pathway when the valves were switched on or off, respectively. Dashed lines in the valve symbols V<sub>5</sub>, V<sub>6</sub> ... V<sub>11</sub> indicate that are normally closed, therefore permit fluid flow only when they are connected.

 1  
2  
3  
4  
5  
6  
7  
8  
9  
10  
11  
12  
13  
14  
15  
16  
17  
18  
19  
20  
21  
22  
23  
24  
25  
26  
27  
28  
29  
30  
31  
32  
33  
34  
35  
36  
37  
38  
39  
40  
41  
42  
43  
44  
45  
46  
47  
48  
49  
50  
51  
52  
53  
54  
55  
56  
57  
58  
59  
60

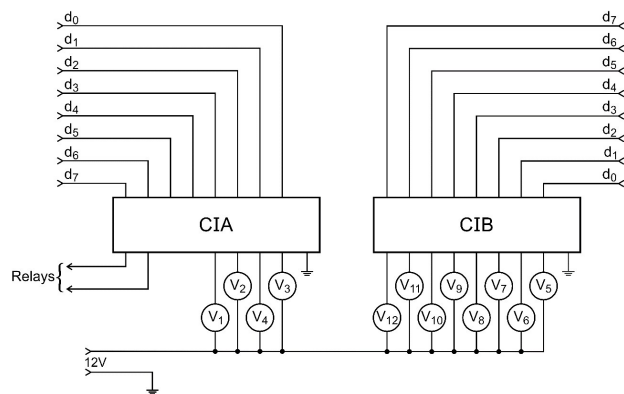


**Figure 3. Diagram of the control interface.** CIA and CIB = integrate circuit ULN2803; V<sub>1</sub>, V<sub>2</sub>, V<sub>3</sub> and V<sub>4</sub> = three-way solenoid valves; V<sub>5</sub>, V<sub>6</sub>, ....., V<sub>12</sub> = solenoid pinch valves normally closed, d<sub>0</sub>, d<sub>1</sub>, .....,d<sub>7</sub> = control lines from the PCL 711 interface card.

1  
2  
3  
4  
5  
6  
7  
8  
9  
10  
11  
12  
13  
14  
15  
16  
17  
18  
19  
20  
21  
22  
23  
24  
25  
26  
27  
28  
29  
30  
31  
32  
33  
34  
35  
36  
37  
38  
39  
40  
41  
42  
43  
44  
45  
46  
47  
48  
49  
50  
51  
52  
53  
54  
55  
56  
57  
58  
59  
60



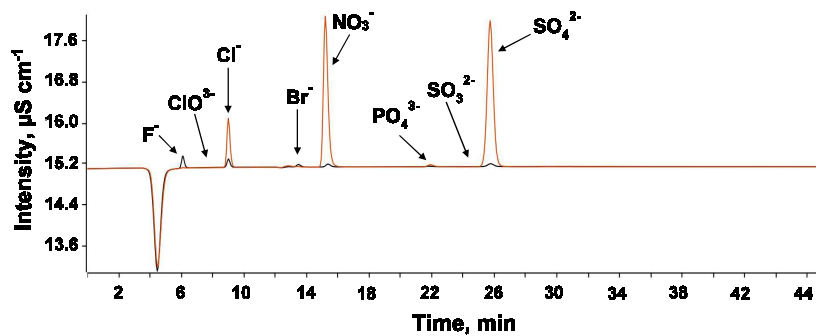


**Figure 4. Chromatogram record of a coke sample after digestion by MIC.** Black line represents the retention time obtained from standard solution. Red line represents the retention time obtained from sample after MIC digestion.

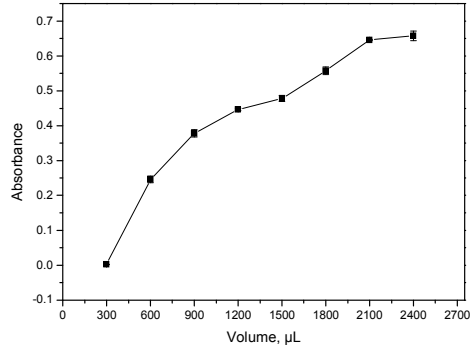


**Figure 5. Effect of the sample zone volume.** Assay carried out using a  $50 \text{ mgL}^{-1}$  sulphate and flow rate of  $200 \mu\text{Ls}^{-1}$ .

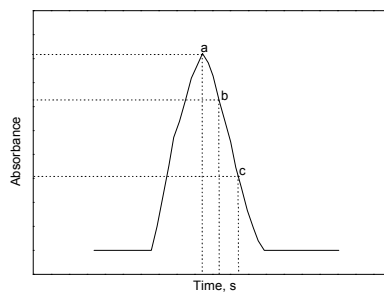


**Figure 6. Record of the transient signal.** Record referred to  $200 \text{ mgL}^{-1}$  sulphate standard solution and settling three sampling cycles. Other parameters as described before.

1  
2  
3  
4  
5  
6  
7  
8  
9  
10  
11  
12  
13  
14  
15  
16  
17  
18  
19  
20  
21  
22  
23  
24  
25  
26  
27  
28  
29  
30  
31  
32  
33  
34  
35  
36  
37  
38  
39  
40  
41  
42  
43  
44  
45  
46  
47  
48  
49  
50  
51  
52  
53  
54  
55  
56  
57  
58  
59  
60

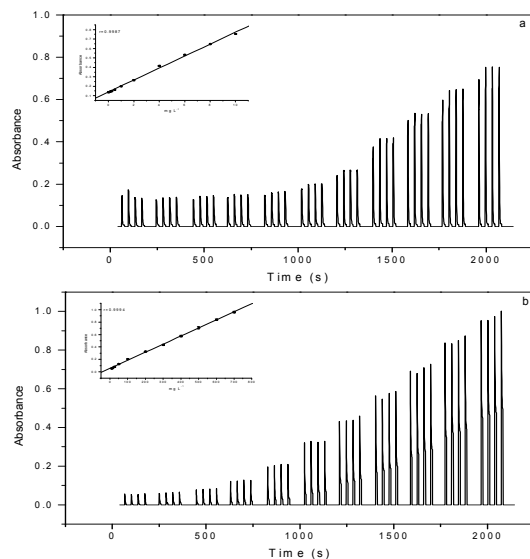


**Figure 7. Records of the transient signals generated simultaneously.** The set of record labeled as *a* correspond to chloride standard solutions of 0.0, 0.06, 0.125, 0.25, 0.5, 1.0, 2.0, 4.0, 6.0, 8.0, 10.0 mg L<sup>-1</sup>, while the other one labelled as *b* is related with sulphate standard solutions of 10, 15, 25, 50, 100, 200, 300, 400, 500, 600, 700 mg L<sup>-1</sup>.